QUADRATURE ALGORITHMS: ELEMENTARY PRINCIPLES TO MULTI-DIMENSIONS

RHEA VARMA

Abstract

This expository paper introduces basic principles of numerical integration. It details the scenarios in which each principle is employed, how they are utilized, and the errors generated by each principle. The paper provides an overview on the core quadrature methodology. It explores numerous quadrature rules and variants, and their formulae. Going past quadrature on a one-dimensional plane, this paper explores numerical integration in a multidimensional plane.

Acknowledgements

The author is greatly indebted to Simon Rubinstein-Salzedo, of the Euler Circle, for providing them with the opportunity to write this paper, giving them this topic of research, and instructing and guiding them on mathematical writing. They are also incredibly grateful to Pariya Akhiani, for mentoring and giving counsel to them, for helping them with and clearing all their queries, and without whom the writing of this paper would not have been possible.

Contents

Date: June 2023.

I Introduction

I.I What is a Quadrature

A method utilized to approximate a definite integral, $\int_a^b f(x)\,dx$ numerically or analytically. A quadrature is additionally defined as a method of squaring. It is the construction of a square figure with the utilization of a compass and straight edge device, to produce a figure with the exact area of the shape itself. The area of a plane geometric figure can be calculated by dividing the figure into an array of shapes (not necessarily squares) with known areas and then determining the limit of the sum of the areas of the shapes.

I.II Methodological Overview

This method of numerical integration requires the selection followed by the evaluation of abscissa on the integrand $f(x)$, which produces an approximation for the value of the definite integral. Different methods of quadrature integration entail the use of different weights, and the selection of the method of quadrature integration in addition to the selection of the optimum points for quadrature should be on the basis of the nature of the integrand $f(x)$ in order to provide the most accurate value for the approximation of the definite integral. All quadrature methods have the same basic structure: the multiplication of a quadrature weight by the sum of the evaluated integrand at certain abscissa.

$$\begin{aligned}\int_a^b f(x)\,dx &\approx w_1 f(p_1) + w_2 f(p_2) + \cdots + w_n f(p_n) \\ &= \sum_{i=1}^{n} f(p_i) w_i \end{aligned} \tag{1}$$

where p_i = quadrature point, n = number of abscissa, w_i = weight

.

The complexity, and henceforth the method of quadrature integration utilized for a certain integrand is dependant on a) the dimension and b) the smoothness of the integrand.

II Elementary Rules

II.I Rectangular Rule

(a) A numerical integration method which approximates the integral of a function using a rectangle. The rectangles are utilized to find the area under the curve. This rule is used for piecewise constant approximation.

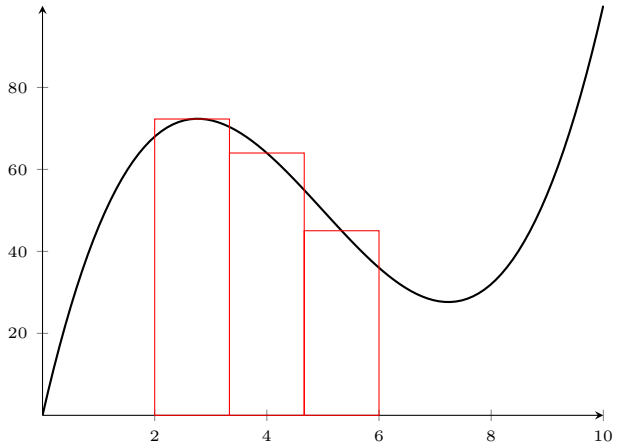

Figure II.I: *An approximation for the integral of a function using the rectangular rule*

(b) For the rectangle rule, the interpolatory function must be a polynomial of degree zero, which passes through ($\frac{a+b}{2}$, f($\frac{a+b}{2}$)), as denoted on Figure II.I.

- Assume the function to be integrated as:

$$\int_a^b f(x)\,dx$$

- Then one must divide the interval $[a, b]$ into m sub-intervals. The width of the rectangles used is based on the interval of integration. Either a single rectangle could be utilized to span across the width of the entire interval of integration, or the interval can divided into m sections of the same length, and therefore m number of rectangles would be used in approximation, with each rectangle having the width of the smaller sub-interval. Each of the sub-intervals is of equal length $h = \frac{b-a}{m}$
- In each sub-interval, one approximates the value of f by $f(x_j^*)$, which applies the midpoint rule over the sub-interval, x_j^* here being used to denote the midpoint.

  For example, x_1^* would be calculated as:

$$x_1^* = a + \frac{b-a}{2m} \tag{2}$$

  x_2^* as:

$$x_2^* = x_1^* + \frac{b-a}{m} \tag{3}$$

  x_3^* as:

$$x_2^* = x_1^* + 2\frac{b-a}{m} \tag{4}$$

  and so on. Until:

$$x_m^* = x_1^* + (m-1)\frac{b-a}{m} \tag{5}$$

- The area of each rectangle becomes $f(x_1^*)h, f(x_2^*)h, f(x_3^*)h, \ldots, f(x_m^*)h$
- Therefore the integration is calculated as

$$\int_a^b f(x)\,dx \approx f(x_1^*)h + f(x_2^*)h + f(x_3^*)h + ... + f(x_m^*)h \tag{6}$$

$$\approx h[f(x_1^*) + f(x_2^*) + f(x_3^*) + ... + f(x_m^*)] \tag{7}$$

- As a greater number of rectangles is used, the value of approximation becomes more accurate, since each rectangle becomes thinner, and its height becomes a better representation of the value of the the function in the interval (the height of the rectangle is the value of the function at the midpoint of its base)

$$\int_a^b f(x)\,dx = \lim_{h\to 0} h[f(x_1^*) + f(x_2^*) + f(x_3^*) + ... + f(x_m^*)] \tag{8}$$

$n \to \infty$ as $h \to 0$, since $h = \frac{b-a}{m}$ and $(b-a)$ is a constant

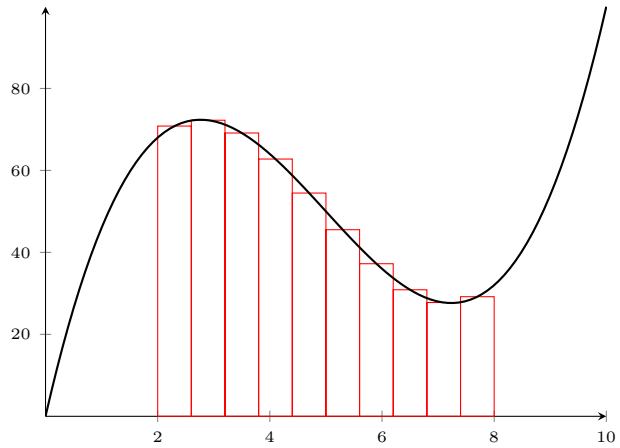

(c) Error Analysis of the Rectangle Rule
As polynomial interpolation is used in the approximation of definite integrals, the error can be calculated using the error formula for polynomial interpolation. The error, E, can be written as:

$$E = \int_a^b f(t)\,dt \; - \int_a^b p(t)\,dt \; = \int_a^b f(t) - p(t)\,dt \tag{9}$$

Furthermore, the error formula for the interpolation over (n+1) points brings E to be:

$$E = \int_a^b f(t) - p(t)\,dt \tag{10}$$

$$= \int_a^b \frac{f^{n+1}(c)}{(n+1)!}(t-x_0)(t-x_1)(t-x_2)...(t-x_n)\,dt \tag{11}$$

$$= \int_a^b \frac{f^{n+1}(c)}{(n+1)!}\prod_{i=0}^{n}(t-x_i)\,dt \tag{12}$$

Let $(t-x_0)(t-x_1)(t-x_2)...(t-x_n)$ be ω(t)
Now we consider the case:

$$\omega(t)\big|_{[a,b]} \geq 0 \text{ or}$$

$$\omega(t)\Big|_{[a,b]} \leq 0 \tag{13}$$

The rectangle rule is evidently an example of this case, as $\omega(t) = t - a$ always proves to be positive. Henceforth, the rectangle rule can be displayed as:

$$E = \frac{f^{n+1}(c)}{(n+1)!}\int_a^b \omega(t)\,dt \tag{14}$$

$$= f'(c)\int_a^b (t-a)\,dt \tag{15}$$

$$= \frac{f'(c)}{2}\cdot(b-a)^2 \tag{16}$$

The interval $(b-a)$, as showcased above, is to the the power of 2. The higher the power it is raised to, the error greatly decreases as the width of the interval does.

II.II Trapezoidal Rule

(a) A numerical integration method which approximates the integral of a function using a trapezoid. The area under the curve is evaluated by dividing this area into smaller trapezia. This rule is used for piecewise linear approximation.

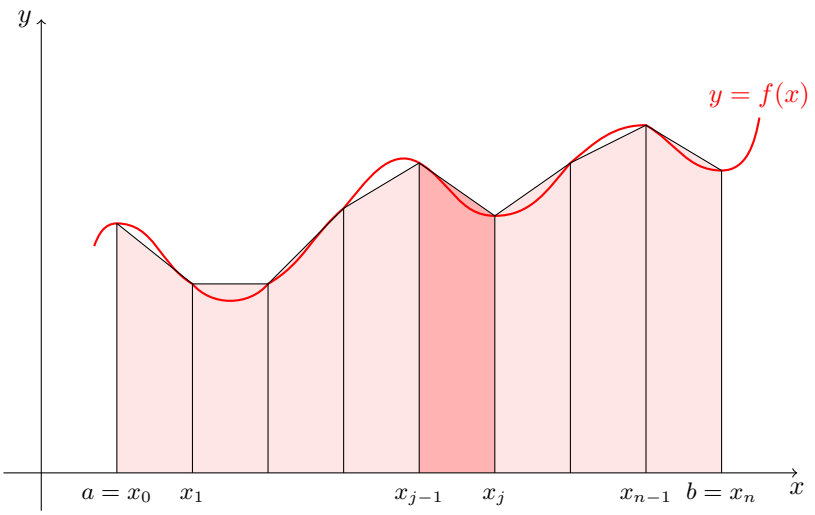

Figure II.II: *An approximation for the integral of a function using the trapezoidal rule*

(b) For the trapezoidal rule, the interpolatory function must be a polynomial of degree one (a straight line) which passes through $(a, f(a))$ and $(b, f(b))$

- Assume the function to be integrated as:

$$\int_a^b f(x)\,dx$$

- One must divide the interval $[a, b]$ into m sub-intervals, each of equal length $h = \frac{b-a}{m}$
- The sum of the area of these m trapezia provides an approximation for the area under the curve.

The area of the first trapezium can be found by adding the area of the triangle and of the rectangle

$$A_1 = \text{area of triangle} + \text{area of rectangle}$$

$$= \frac{1}{2}[f(x_1) - f(a)] + f(a)h \tag{17}$$

$$= \frac{1}{2}h[f(a) + f(x_1)] \tag{18}$$

The area of the second can be calculated as:

$$A_2 = \frac{1}{2}h[f(x_1) + f(x_2)] \tag{19}$$

The area of the third can be calculated as:

$$A_3 = \frac{1}{2}h[f(x_2) + f(x_3)] \tag{20}$$

The area of the penultimate trapezium can be calculated as:

$$A_P = \frac{1}{2}h[f(x_{m-2}) + f(x_{m-1})] \tag{21}$$

And the area of the last trapezium can be calculated as:

$$A_m = \frac{1}{2}h[f(x_{m-1}) + f(b)] \tag{22}$$

Finally, the total area can be approximated as:

$$\int_a^b f(x)\,dx = \frac{1}{2}h[f(a)+f(x_1)+f(x_1)+f(x_2)+\cdots+f(x_{m-2})+f(x_{m-2})+ f(x_{m-1})+f(x_{m-1})+f(b)] \tag{23}$$

$$= \frac{b-a}{m}\left(\frac{f(a)}{2}+\sum_{k=1}^{m-1}(f(a)+k\left(\frac{b-a}{m}\right)\right)+\frac{f(b)}{2} \tag{24}$$

(c) Error Analysis of the Trapezoidal Rule
Like the rectangle rule, the trapezoidal rule is too an evident example of the case displayed in (13), as $\omega(t) = (t-a)(t-b)$. From a to b, $\omega(t) < 0$, since $(t-b) < 0$ and $(t-a) > 0$.
The error for the trapezoidal rule can be written as:

$$E_T = \frac{f''(c)}{2}\int_a^b (t-a)(t-b)\,dt \tag{25}$$

$$= \frac{f''(c)}{2}\cdot\left(-\frac{(b-a)^3}{6}\right) \tag{26}$$

$$= -\frac{f''(c)}{12}\cdot(b-a)^3 \tag{27}$$

II.III Simpson's Rule

(a) A method of numerical integration used for piecewise quadratic approximation. It approximates the integral of a function by the quadratic interpolant. There are 2 variants, Simpson's 1/3 Rule and Simpson's 3/8 Rule.

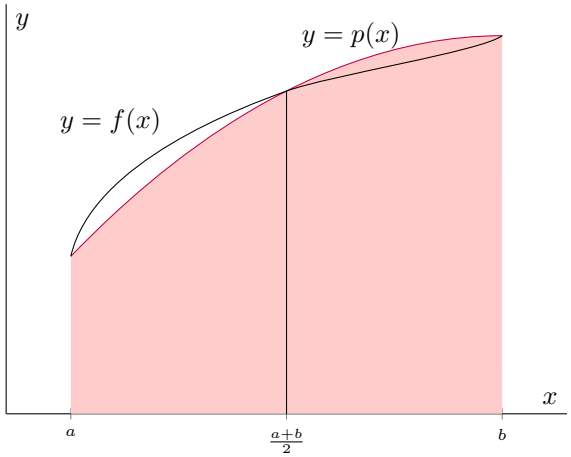

Figure II.III: An approximation of the function $f(x)$ by $p(x)$ using Simpson's rule

II.III.I Simpson's 1/3 Rule

(a) When the 1/3 rule is applied to m sub-intervals of equal length in the [a,b] interval, weights of 2/3 and 4/3 are alternatively given to points in the interval.
Simpson's 1/3 rule is based on polynomials of degree 2, and can be stated as:

$$\int_a^b f(x)\,dx \approx \frac{1}{3}h[f(a)+4f\left(\frac{a+b}{2}\right)+f(b)] \tag{28}$$

$$\approx \frac{b-a}{6}[f(a)+4f\left(\frac{a+b}{2}\right)+f(b)] \tag{29}$$

Assuming the function to be integrated was

$$\int_a^b f(x)\,dx$$

And h to be

$$h = \frac{b-a}{2}$$

(b) This formula can be derived in two ways, the first making use of the trapezoidal and midpoint rules The trapezoidal rule states

$$T = \frac{1}{2}(b-a)(f(a)+f(b)) \tag{30}$$

And the midpoint rule states

$$M = (b-a)f\left(\frac{a+b}{2}\right) \tag{31}$$

The weighted average of these formulae, $\frac{T+2M}{3}$, gives us the Simpson's 1/3 rule.
The second way to derive Simpson's 1/3 rule is to replace the function, $f(x)$, with a quadratic polynomial, $p(x)$, which uses the values at the beginning and end of the interval, a and b respectively, and the midpoint of these two values.
$p(x)$ can be calculated using a Lagrangian Interpolating Polynomial, as shown below:

$$p(x) = f(a)\frac{(x-m)(x-b)}{(a-m)(a-b)} + f(m)\frac{(x-a)(x-b)}{(m-a)(m-b)} + f(b)\frac{(x-a)(x-m)}{(b-a)(b-m)} \tag{32}$$

by integrating the polynomial we find that:

$$\int_a^b f(x)\,dx = \frac{b-a}{6}[f(a)+4f\left(\frac{a+b}{2}\right)+f(b)] \tag{33}$$

$$= \frac{1}{3}h[f(a)+4f\left(\frac{a+b}{2}\right)+f(b)] \tag{34}$$

where

$$h = \frac{b-a}{2}$$

When there is an oscillatory interval of integration, the interval must be broken up into many smaller intervals. Simpson's 1/3 rule must them be applied over each of these sub-intervals, and then these values added together in order to provide a value for the approximation of the integral.

- Assume the function to be integrated as

$$\int_a^b f(x)\,dx$$

- Divide the interval $[a,b]$ into m sub-intervals, each of equal length $h = \frac{b-a}{m}$
- We next have to introduce the point $x_i = a + ih$, where i is $0 \le i \le m$
- Finally, the integral can be approximated as:

$$\int_a^b f(x)\,dx \approx \frac{1}{3}h\sum_{i=1}^{\frac{m}{2}}[f(x_{2i-2})+4f(x_{2i-1})+f(x_{2i})] \tag{35}$$

$$\approx \frac{1}{3}h[f(x_0)+4f(x_1)+2f(x_2)+4f(x_3)+2f(x_4)+...+4f(x_{m-1})+f(x_m)] \tag{36}$$

$$\approx \frac{1}{3}h[f(x_0)+4\sum_{i=1}^{\frac{m}{2}}f(x_{2i-1})+2\sum_{i=1}^{\frac{m}{2}-1}f(x_{2i})+f(x_m)] \tag{37}$$

II.III.II Simpson's 3/8 Rule

(a) Simpson's 3/8 rule can be stated as:

$$\int_a^b f(x)\,dx \approx \frac{3}{8}h[f(a)+3f\left(\frac{2a+b}{3}\right)+3f\left(\frac{a+2b}{3}\right)+f(b)] \tag{38}$$

$$\approx \frac{b-a}{8}[f(a)+3f\left(\frac{2a+b}{3}\right)+3f\left(\frac{a+2b}{3}\right)+f(b)] \tag{39}$$

Assuming the function to be integrated was

$$\int_a^b f(x)\,dx$$

And h to be

$$h = \frac{b-a}{3}$$

(b) Simpson's 3/8 rule uses cubic interpolation, unlike Simpson's 1/3 rule, which uses quadratic interpolation.

- Assume the function to be integrated as

$$\int_a^b f(x)\,dx$$

- Divide the interval $[a, b]$ into m sub-intervals, each of equal length $h = \frac{b-a}{m}$
- We next have to introduce the point $x_i = a + ih$, where i is $0 \leq i \leq m$
- Finally, the integral can be approximated as:

$$\int_a^b f(x)\,dx \approx \frac{3}{8}h\sum_{i=1}^{\frac{m}{3}}[f(x_{3i-3}) + 3f(x_{3i-2}) + 3f(x_{3i-1}) + f(x_{3i})] \tag{40}$$

$$\approx \frac{3}{8}h[f(x_0) + 3f(x_1) + 3f(x_2) + 2f(x_3) + 3f(x_4) + 3f(x_5) + 2f(x_6)... + 3f(x_{m-1}) + f(x_m)] \tag{41}$$

$$\approx \frac{3}{8}h[f(x_0) + 3\sum_{i=1}^{m-1} f(x_i) + 2\sum_{i=1}^{\frac{m}{3}-1} f(x_{3i}) + f(x_m)] \tag{42}$$

II.III.III Proving Simpson's Rule

Proof. Consider the area under a parabola y with equation $y = ax^2 + bx + c$

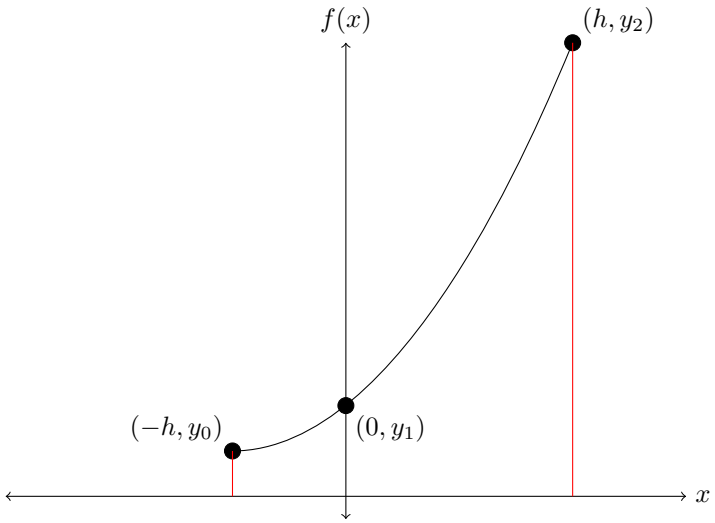

If we integrate the area enclosed within the red lines above, we get:

$$\int_{-h}^{h}(ax^2 + bx + c)\,dx = \left[\frac{ax^3}{3} + \frac{bx^2}{2} + cx\right]_{-h}^{h} \tag{43}$$

$$= (\frac{ah^3}{3} + \frac{bh^2}{2} + ch) - (-\frac{ah^3}{3} + \frac{bh^2}{2} - ch) \tag{44}$$

$$= \frac{2ah^3}{3} + 2ch \tag{45}$$

$$= \frac{h}{3}(2ah^2 + 6c) \tag{46}$$

The parabola passes through $(-h, y_0)$, $(0, y_1)$ and (h, y_2). If we substitute these points into $y = ax^2 + bx + c$, we obtain the equations

$$y_0 = ah^2 - bh + c \tag{47}$$

$$y_1 = c \tag{48}$$

$$y_2 = ah^2 + bh + c \tag{49}$$

From these equations, we can deduce that:

$$c = y_1 \tag{50}$$

and

$$2ah^2 = y_0 - 2y_1 + y_2 \tag{51}$$

which is the sum of equation (1) and (3) By substituting these equations into $A = \frac{h}{3}(2ah^2 + 6c)$, we have

$$A = \frac{h}{3}(2ah^2 + 6c) \tag{52}$$

$$= \frac{h}{3}(y_0 - 2y_1 + y_2 + 6y_1) \tag{53}$$

$$= \frac{h}{3}(y_0 + 4y_1 + y_2) \tag{54}$$

Now, we can consider the area of the parabola for the next 3 points:

$$A = \frac{h}{3}(y_2 + 4y_3 + y_4) \tag{55}$$

Adding the 2 areas together, we obtain:

$$A = \frac{h}{3}(y_0 + 4y_1 + 2y_2 + 4y_3 + y_4) \tag{56}$$

If we keep going, we finally arrive at Simpson's rule:

$$\int_a^b f(x)\,dx \approx \frac{h}{3}(y_0 + 4y_1 + 2y_2 + 4y_3 + 2y_4 + ... + 4y_{n-1} + y_n) \tag{57}$$

□

II.III.IV Error Analysis of the Simpson's rule

For the Simpson's rule, we consider the case

$$\int_a^b \omega(t)\,dt = 0$$

The definite integral of the next Newton polynomial in the interval will equal 0. Therefore, adding a point to the interpolation will not affect the value of the approximation of the integral produced. The error can be calculated by adding another point to the polynomial interpolation. To carry out the error finding, one must double the midpoint so the node set equates to:

$$X = \{a, \frac{a+b}{2}, \frac{a+b}{2}, b\} \tag{58}$$

The subsequent Newton polynomial can be written as:

$$\omega(t) = (t-a)(t-b)\left(t - \frac{a+b}{2}\right)^2 \tag{59}$$

Since $\omega(t)\big|_{[a,b]} \leq 0$,

$$E_S = \frac{f^{(4)}(c)}{24} \int_a^b (t-a)(t-b\left(t - \frac{a+b}{2}\right)^2 \, dt \tag{60}$$

$$= \frac{f^{(4)}(c)}{2880}(b-a)^5 \tag{61}$$

II.IV Lagrange Interpolation

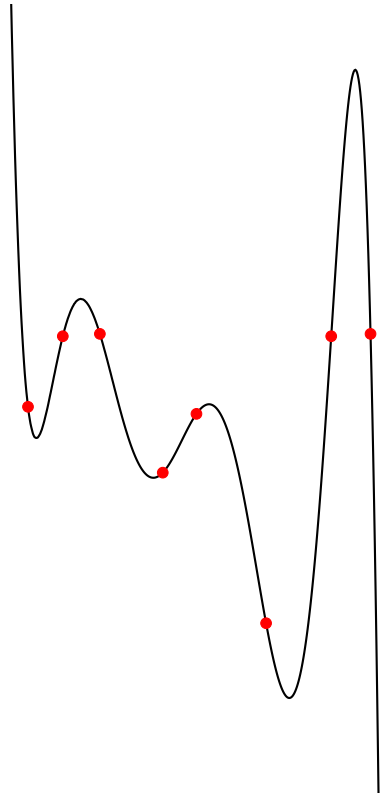

Figure II.IV: *A Lagrange interpolating polynomial (black line) passing through the points* marked.

A Lagrange interpolating polynomial is a polynomial which passes through m points, and is of the degree $\leq (m-1)$.

The greater the value of m, the greater the degree of the Lagrange interpolating polynomial. There will be greater oscillation between points, meaning a worse approximation of the function between them, but greater accuracy at the points. The polynomial is calculated as:

$$p(x) = \frac{(x-x_2)(x-x_3)...(x-x_m)}{(x_1-x_2)(x_1-x_3)...(x_1-x_m)}y_1 + \frac{(x-x_1)(x-x_3)...(x-x_m)}{(x_2-x_1)(x_2-x_3)...(x_2-x_m)}y_2 +$$

$$... + \frac{(x-x_1)(x-x_2)...(x-x_{m-1})}{(x_m-x_1)(x_m-x_2)...(x_m-x_{m-1})}y_m \tag{62}$$

and simply displayed as:

$$p(x) = \sum_{j=1}^{n} p_i(x) \tag{63}$$

where

$$p_i(x) = y_i \prod_{k=1,\neq i}^{n} \frac{x-x_k}{x_i-x_k} \tag{64}$$

Allow $p(x)$ to be a polynomial of degree n, with 0s appearing at x_1 and x_n. The fundamental polynomial can be written as:

$$p_\nu(x) = \frac{p(x)}{p'(x_\nu)(x - x_\nu)} \tag{65}$$

where

$$p_\nu(x_\mu) = \delta_{\nu\mu} \tag{66}$$

$\delta_{\nu\mu}$ denotes what is known as the Kronecker's delta. This means

$$\delta_{\nu\mu} = \begin{cases} 1 & \text{if } \nu = \mu, \\ 0 & \text{if } \nu \neq \mu. \end{cases}$$

We now consider the values of $y_1 \dots y_n$, then

$$P_n(x) = \sum_{\nu=1}^{n} y_\nu l_\nu(x) \tag{67}$$

We now consider $l_1(x), \dots, l_n(x)$, the fundamental polynomials, the corresponding orthogonal polynomial,$p_n(x)$, and an arbitary distribution $d\alpha(x)$ on the interval of $[a, b]$

$$\int_a^b l_\nu(x) l_\mu(x) d\alpha(x) \ = \lambda_\mu \delta_{\nu\mu} \tag{68}$$

for $\nu, \mu = 1$, 2, ..., n, where λ_ν are known as the Christoffel Numbers.

III Quadrature Types

Integrals may be in mutli-dimensional spaces, have complex boundaries, be highly oscillatory, badly behaved functions, or we may only know the integrand at a few points. This makes the integral extremely hard to solve. Quadrature is method utilized to approximate a definite integral,

$$\int_a^b f(x)\, dx$$

either by numerical methods and even analytically, when possible. Using quadrature, we deduce the area bounded by a curve, by making close approximations through the use of carefully selected abscissae and weighting functions.

III.I Gaussian Quadrature

The Gaussian method of numerical integration involves the selection of optimum quadrature points on a curve at which to evaluate the function. A suitable weight is selected for the points, and this weight is then applied across this abscissa. The sum of these points with their applied weights produces a value for the approximation of the definite integral. Gaussian quadrature is designed for polynomials of degree $\leq (2n - 1)$. Selecting the right points within the interval $[a, b]$ is crucial in providing the most accurate result.

III.I.I Gauss-Legendre Quadrature

The interval for integration in this rule is most commonly $[-1, 1]$ and the rule can be displayed as

$$\int_{-1}^{1} f(x)\, dx \ \approx \sum_{i=1}^{m} w_i f(x_i)$$

where w_i = weight, m = number of abscissa x_i = roots of the mth Legendre polynomial

The polynomial utilized in Gauss-Legendre is the Legendre polynomial, a type of orthogonal polynomial. Orthogonal polynomials are a set of polynomials defined over a fixed range which follow orthogonality relations. Assuming the Legendre polynomial to be denoted by $P_m(x)$, the quadrature points are the roots of $P_m(x)$ and the weights can be displayed as:

$$w_i = \frac{A_m}{A_{m-1}} \frac{\gamma_{m-1}}{P_{m-1}(x_i) P'_m(x_i)} \tag{69}$$

where A_m is the coefficient of x^m in the polynomial $P_m(x)$, and can be denoted as:

$$A_m = \frac{(2m)!}{2^m(m!)^2} \tag{70}$$

Henceforth,

$$\frac{A_{m+1}}{A_m} = \frac{2(m+1)!}{2^{m+1}[(m+1)!]^2}\frac{2^m(m!)^2}{(2m)!} \tag{71}$$

$$= \frac{2m+1}{m+1} \tag{72}$$

w_i can be written as:

$$w_i = \frac{2(1-x_i^2)}{(m+1)^2[P_{m+1}(x_i)]^2} \tag{73}$$

γ_m can be written as:

$$\int_{-1}^{1}[P_m(x)]^2\ dx = \frac{2}{2m+1} \tag{74}$$

III.I.II Gauss-Jacobi Mechanical Quadrature

The interval for integration in this rule is most commonly $[-1, 1]$ and the rule can be displayed as:

$$\int_{-1}^{1}(1-x)^\alpha(1+x)^\beta f(x)\ dx = \sum_{i=1}^{m} w_i f(x_i) + E \tag{75}$$

The polynomial utilized in Gauss-Jacobi is the Jacobi polynomial, a type of orthogonal polynomial. Assuming the Jacobi polynomial to be denoted by $P_m(x)$, the quadrature points are the roots of $P_m(x)$ and the weights can be displayed by:

$$w_i = -\frac{2m+\alpha+\beta+2}{m+\alpha+\beta+1}\frac{\Gamma(m+\alpha+1)\Gamma(m+\beta+1)}{\Gamma(m+\alpha+\beta+1)(m+1)!}\frac{2^{\alpha+\beta}}{P_m^{(\alpha,\beta)'}(x_i)P_{m+1}^{(\alpha,\beta)}(x_i)} \tag{76}$$

and where E can be written as:

$$E = \frac{\Gamma(m+\alpha+1)\Gamma(m+\beta+1)\Gamma(m+\alpha+\beta+1)}{(2m+\alpha+\beta+1)[\Gamma(2m+\alpha+\beta+1)]^2}\frac{2^{2m+\alpha+\beta+1}m!}{(2m)!}f^{(2m)} \tag{77}$$

III.I.III Gauss-Kronod Quadrature

The Gauss-Kronod method is a nested quadrature rule. A nested quadrature is one in which two orders of rules, higher order and lower order, both exist for a set of abscissa. There are two calculations carried out for the approximation of the value of the definite integral. One, more accurate, and the other, less accurate. The more accurate approximation is calculated from the information provided by the calculation of the less accurate approximation. The quadrature points of a Gauss-Kronod quadrature, known as the Kronod points, are chosen so that this approximation can be carried out. The difference between the higher and lower order approximation provides the error. Assume the function to be integrated as

$$\int_a^b f(x)\,dx$$

This can be evaluated using the standard Gaussian quadrature. The Gauss-Kronod is a slight modification of the Gaussian quadrature, turning the m-point rule into one of order $3m+1$ upon the addition of $m+1$ points to the characteristic $2m-1$ order Gaussian rule. The additional points which are generated are the zeros of what are known as Stieltjes polynomials, a type of orthogonal polynomial. These additional points enable the calculation of the high order approximation, with the use of the results of the low order approximation as well. The error for the approximation of the definite integral can be found by calculating the difference between the Gaussian rule and its Gauss-Kronod variation. The Gauss-Kronod quadrature can be displayed as:

$$\int_{-1}^{1} f(x)\ dx = \sum_{i=1}^{m} A_i^{(m)} f(\xi_i^{(m)}) + \sum_{j=1}^{m+1} B_j^{(m)} f(x_j^{(m)}) + R_K^{(m)}(f) \tag{78}$$

where $\xi_i^{(m)}, i = 1, \ldots, m$ are the zeros of the polynomial, $A_i^{(m)}$ and $B_j^{(m)}$ are the weights and $x^(m)_j$ are the nodes selected in order to produce the degree of $3m + 1$.

III.I.IV Gauss-Hermite Quadrature

The Gauss-Hermite quadrature is utilized when the domain is infinite and the function has singularities at both ends. It can be used to evaluate functions of the following kind

$$\int_{-\infty}^{\infty} e^{-x^2} f(x)\ dx$$

to produce the rule:

$$\int_{-\infty}^{\infty} e^{-x^2} f(x)\ dx = \sum_{k=1}^{m} H_k f(x_k) + E \tag{79}$$

where

$$H_i = -\frac{2^{m+1} m! \sqrt{\pi}}{H'_m(x_i) H_{m+1}(x_i)} = \frac{2^m (m-1)! \sqrt{\pi}}{H'_m(x_i) H_{m-1}(x_i)} \tag{80}$$

$H'_m(x_i)$ being

$$H'_m(x_i) = 2m H_{m-1}(x_i) = -H_{m+1}(x_i) \tag{81}$$

and where E can be displayed by

$$E = \frac{m! \sqrt{\pi}}{2^m (2m)!} f^{(2m)(\xi)} \tag{82}$$

for some ξ

III.I.V Gauss-Laguerre Quadrature

The Gauss-Laguerre bears similarity to the Gauss-Hermite quadrature, except it goes over an interval of $[0, \infty]$, and has a weight of e^{-x} The polynomial utilized in Gauss-Laguerre is the Laguerre polynomial, a type of orthogonal polynomial. The roots of this polynomial provide the quadrature points for evaluation. The weights can be displayed as:

$$w_i = -\frac{A_{m+1} \gamma_m}{A_m L'_m(x_i) L_{m+1}(x_i)} \tag{83}$$

$$= \frac{A_m}{A_{m-1}} \frac{\gamma_{m-1}}{L_{m-1}(x_i) L'_m(x_i)} \tag{84}$$

where

$$\gamma_m = \int_0^{\infty} W(x) [L_m(x)]^2\ dx = 1 \tag{85}$$

and where A_m denotes the coefficient of x_m in the Laguerre polynomial.

III.II Radau Quadrature

The Radau quadrature is quite similar to the Gaussian quadrature, and only provides slightly less accuracy. It too fits all polynomials of degree $2m - 1$, though originally designed to fit polynomial of degree $2m$. It integrates over a finite interval, with a unit weighting function, $W(x)$. When an end of the interval becomes assigned to be a quadrature point, we can assume the interval was changed to be $[-1, 1]$, with the fixed point being -1. Radau quadrature can be obtained by:

$$F(\mu) = (1 - \mu^2) P'_m(\mu) \tag{86}$$

This equation makes it evident that (μ_j) will have $(m + 1)$ abscissa, with $\mu = \pm 1$ and $(m - 1)$ zeros of the polynomial.
The Christoffel numbers can be written as:

$$\lambda_j = \frac{1}{m(m+1)} [P_m(\mu_j)]^{-2} \tag{87}$$

$F(\mu)$ can also be written in the form:

$$F(\mu) = \frac{m(m+1)}{2m+1} [P_{m-1}(\mu) - P_{m+1}(\mu)] \tag{88}$$

We can therefore deduce that:

$$\int_{-1}^{1} F(\mu)\mu^{l} \ = 0, \ l \leq (m-2) \tag{89}$$

As $F(\mu)$ is of degree $m+1$, a quadrature rule based on the zeros of $F(\mu)$ will provide an acute approximation for integrals of the form $\int_{-1}^{1} F(\mu)\ d\mu$ for all polynomials of degree $\leq (2m-1)$. Simply, Radau quadrature provides the accuracy of a Gaussian quadrature of m points using $m+1$ points.
Radau quadrature can finally be written as:

$$\int_{-1}^{+1} f(\mu)\ d\mu \approx \frac{1}{m(m+1)} \sum_{j=1}^{m+1} \frac{f(\mu_j)}{[P_m(\mu_j)]^2} \tag{90}$$

III.III Clenshaw-Curtis Quadrature

Clenshaw-Curtis evaluates $m+1$ points to a degree of m, whereas Gaussian quadrature is designed to evaluate $m+1$ points, of degree $\leq (m-1)$. While it does not appear so, the Clenshaw-Curtis quadrature provides accuracy equal to that of a Gaussian quadrature.

Clenshaw-Curtis depends on the expansion of the function through the use of Chebyshev polynomials, and a change of variables, specifically $x = cos\theta$, and approximation through discrete cosine transformation (DCT). It integrates function over an interval of $[-1, 1]$. DCT represents a set of data using a sum of cosine functions at various frequencies. Clenshaw-Curtis results in nested quadrature, in which the same abscissa are utilized for two orders of approximation. The quadrature points at which the function is approximated are the roots of the Chebyshev polynomial, and these values are utilized to evaluate the integral with complete accuracy. The weights utilized are computed beforehand using what is known as a Fast Fourier transform. The key of the Clenshaw-Curtis is the variable change, which can be displayed as:

$$\int_{-1}^{1} f(x)\, dx = \int_{0}^{\pi} f(\cos\theta)\sin(\theta)\, d\theta \tag{91}$$

Carrying out this integration is possible if we can calculate the cosine series for the function. The cosine series for an even function of f with a period $2L$ can be displayed as

$$f(x) = \frac{c_0}{2} + \sum_{n=1}^{\infty} \frac{2}{L} \int_{0}^{L} f(x) cos\frac{n\pi x}{L}\ dx \cos\frac{n\pi x}{L} \tag{92}$$

The cosine series of $f(cos\theta)$ can be written as:

$$f(cos\theta) = \frac{a_0}{2} + \sum_{n=1}^{\infty} a_k cos(k_0) \tag{93}$$

which means that the function can be integrated as:

$$\int_{0}^{\pi} f(cos\theta) sin(\theta)\ d\theta = a_0 + \frac{2a_{2k}}{1-(2k)^2} \tag{94}$$

Fourier-series integration for a periodic function upto n points (known as the Nyquist frequency) can be accurately computed using $n+1$ points of equal spacing and equal weighting. Rather than performing numerical integration once again, we use a DCT transform to evaluate the integrand, as displayed below:

$$a_{2k} \approx \frac{2}{N}\left[\frac{f(1)+f(-1)}{2} + f(0)(-1)^k + \sum_{n=1}^{N/2-1} \{f(\cos[n\pi/N]) + f(-\cos[n\pi/N])\} \cos\left(\frac{nk\pi}{N/2}\right)\right] \tag{95}$$

This is the most commonly used methodology of Clenshaw-Curtis.

III.IV Cavalieri Quadrature Formula

Caliaveri's quadrature can be written as:

$$\int_0^a x^n \, dx = \tfrac{1}{n+1} \, a^{n+1} \tag{96}$$

For $n \geq 0$ When x is raised to a negative power, a singularity generates at $x = 0$, resulting in:

$$\int_1^a x^n \, dx = \frac{1}{n+1}(a^{n+1} - 1) \tag{97}$$

where $n \neq -1$. A special case originates when $n = -1$, in which case the integrand is converted to a logarithm.

$$\int_1^a \frac{1}{x} \, dx = \ln a \tag{98}$$

$$= \int lnx + cdx \tag{99}$$

Cavalieri proved his formula as follows:
The integral of x^n is taken, which equates to nx^{n-1}. This value can then be geometrized. We assume x^n to be the volume of an n-cube. The derivative therefore becomes equal to the change in volume as the length along the sides undergoes a change. This value can be written as x^{n-1}, which can be interpreted as the area of n faces, each with a dimension of $n - 1$. Alternatively, the geometrisation of the fundamental calculus theorem, the stacking of $n - 1$ cubes forms a pyramid in result, and an n number of these pyramids will result in the formation of an n cube, thus proving the formula.

III.V Chebyshev Quadrature

In the Chebyshev quadrature, all weights are equal. This quality makes the Chebyshev quadrature far more efficient than the Gaussian quadrature, and significantly minimizes error in comparison. The quadrature points are the roots of the Chebyshev polynomial, an orthagonal polynomial associated with the Chebyshev quadrature. Assume the interval of the function to have been transformed to $[-1, 1]$, so that the rule can be written as:

$$\int_{-1}^{1} f(x)w(x) \, dx = W \sum_{k=1}^{m} f(x_k) + E[f(x)] \tag{100}$$

Chebyshev evaluates integrals of two kinds: Firstly:

$$\int_{-1}^{+1} \frac{f(x)}{\sqrt{1-x^2}} \, dx$$

This solves as displayed below:

$$\int_{-1}^{+1} \frac{f(x)}{\sqrt{1-x^2}} \, dx \approx \sum_{i=1}^{n} w_i f(x_i) \tag{101}$$

where

$$x_i = \cos\left(\frac{2i-1}{2n}\pi\right) \tag{102}$$

The weighting function can be displayed as:

$$w(x) = \frac{1}{\sqrt{1-x^2}} \tag{103}$$

W is dictated by the condition that $f(x) = 1$ and $E = 0$, it can be displayed as:

$$W = \frac{\lambda}{m} \tag{104}$$

where

$$\lambda = \int_{-1}^{1} w(x)dx \tag{105}$$

We now consider $\pi(x)$, the Lagrange interpolating polynomial for the first order Chebyshev polynomial

$$\pi(x) = (x - x_1)(x - x_2) \dots (x - x_m)$$

$f(x)$ can be denoted as the special case:

$$f(x) = \frac{1}{u-x} \tag{106}$$

The quadrature rule can therefore be written as:

$$\int_{-1}^{1} w(x)\frac{dx}{u-x} \ = \frac{\lambda}{m}\sum_{k=1}^{m}\frac{1}{u-x_k} + E\left[\frac{1}{u-x}\right] \tag{107}$$

As the sum in the above equation can be denoted as:

$$\frac{d}{du}\log\pi(u) \tag{108}$$

Finally, the rule becomes:

$$\int_{-1}^{1} w(x)\log(u-x)\ dx = \frac{\lambda}{m}\frac{d}{du}[\log\pi(u)] + E\left[\frac{1}{u-x}\right] \tag{109}$$

III.VI Tanh-Sinh Quadrature

tanh-sinh is a quadrature method utilized in the cases where there is an infinite derivative or a singularity at an end-point of the function (or both end-points). tanh-sinh quadrature is founded on the Euler–Maclaurin formula. It can be used in the approximation of an integral through finite sums, or vice versa. Euler-Maclaurin states that integral of a bell-shaped function can be approximated by a step-wise finite summation, with incredibly high accuracy. tanh-sinh integrates functions of the following structure

$$\int_{-1}^{1} f(x)\ dx$$

by transforming the interval of $[-1, 1]$ to $[-\infty, \infty]$. This change of interval is carried out by a variable substitution of $x = \Psi(t)$ where

$$\Psi(t) = \tanh(\frac{\pi}{2}\cdot \sinh t) \tag{110}$$

$$\Psi(x) \to -1 \text{ as } x \to -\infty,\ \Psi(x) \to 1 \text{ as } x \to \infty$$

For very large positive input, and very large negative input, the derivative nears zero. Hence,

$$\int_{-1}^{1} f(x)\ dx = \int_{-1}^{1} f(\Psi(t))\Psi'(t)\ dt \tag{111}$$

$$\approx h\sum_{i=-N}^{N} w_i f(x_i) \tag{112}$$

Approximating the integral utilizing the trapezoidal rule (refer §II.II) yields the following equation,

$$\lim_{m\to\infty}\sum_{i=-m}^{m} h\Psi'(t_i)f(\Psi(t_i)) \tag{113}$$

where $t_i = ih, i \in \mathbb{R}$

IV The Multi-dimensions

We have, till this point, explored quadrature in a one dimensional plane. To expand into a multidimensional plane, we can utilize what is known as Fubini's theorem. Fubini transforms an integral in a multidimensional plane into a repeated one dimensional integral. However, Fubini's theorem can only work under one condition: as the number of dimensions we work with increase, the function evaluation must grow at a rapid rate. This is what is known as the curse of dimensionality. The methods discussed in this section seek to solve this problem.

IV.I Lebedev Quadrature

Lebedev evaluates the surface area of a three-dimensional sphere. The weights utilized and the number of and which abscissa are to be chosen for evaluation on the grid are determined by carrying out the integration and evaluation of sphere harmonics to a certain order, all with perfect accuracy. Spherical harmonics are a set of functions used to represent functions on the surface of the sphere. Spherical harmonics are the eigenfunctions of the angular part of the Laplacian equation in a three-dimensional space. An eigenfunction is a function in the three-dimensional space, which upon effect of a linear factor, is only mutliplied by what is known as the eigenvalue. The order of a sphere harmonic is determined by the zonal wave number, which is the number of wavelengths which are included within a circular section of the sphere at a certain latitude value.

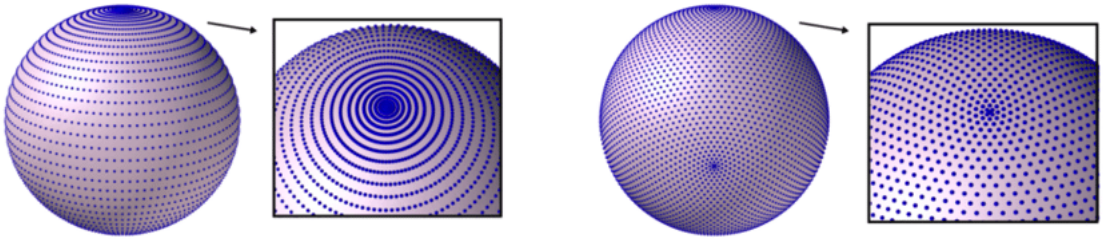

Figure IV.I: *Node distribution in Gauss-Legendre (showcased left), versus Lebedev (showcased right). Image from Hydrodynamic Flows on Curved Surfaces: Spectral Numerical Methods for Radial Manifold Shapes.*

Gauss-Legendre showcases an incredibly dense clusters of points along its latitude nearing the North and South poles of the sphere. Lebedev quadrature has greater symmetry than Gauss-Legendre. Lebedev showcases lower density of points overall, with clustering of the nodes around certain points on the sphere, but not to the degree of Gauss-Legendre.
To integrate over the surface of the sphere, we apply the formula:

$$I[f] = \int \mathrm{d}\Omega\ f(\Omega) = \int_0^{\pi} \sin(\theta)\mathrm{d}\theta \int_0^{2\pi} \mathrm{d}\varphi\ f(\theta,\varphi) \tag{114}$$

Which Lebedev approximated as:

$$\tilde{I}[f] = 4\pi \sum_{i=1}^{N}\ w_i f(\theta_i,\varphi_i) \tag{115}$$

This method is far more efficient than Fubini's theorem. Instead of repeating several one-dimensional integrals, a single sum is utilized to compute the integral of the three-dimesional structure. This means that fewer abscissa are used for the same calculation, with the same accuracy.

In Lebedev quadrature, the grid points are dependant on two factors: the inversion symmetry and octahedral rotation of the grid. The points must be invariant under both these factors. For a given point on the sphere, there are $5, 7, 11, 23$ or 47 points with an identical octahedral group to the given point. A common weighting function is shared between points of the same inversion and rotation. The smallest set of these points is constructed from 6 permutations, and can be displayed in the resulting integration scheme below:

$$\tilde{I}_6[f] = A_1 \sum_{i=1}^{6} f(a_i^1) \tag{116}$$

Continuing this scheme for more sets of points, leads to the complete Lebedev scheme:

$$\tilde{I}_N[f] = A_1 \sum_{i=1}^{6} f(a_i^1) + A_2 \sum_{i=1}^{12} f(a_i^2) + A_3 \sum_{i=1}^{8} f(a_i^3) + \sum_{k=1}^{N_1} B_k \sum_{i=1}^{24} f(b_i^k) + \sum_{k=1}^{N_2} C_k \sum_{i=1}^{24} f(c_i^k) + \sum_{k=1}^{N_3} D_k \sum_{i=1}^{48} f(d_i^k) \tag{117}$$

For an extremely accurate formula, we can integrate the surface of a radial manifold using the manifold metric. The quadrature for the surface area of the radial manifold can be derived using a diffeomorphism, that converts the sphere into a manifold.

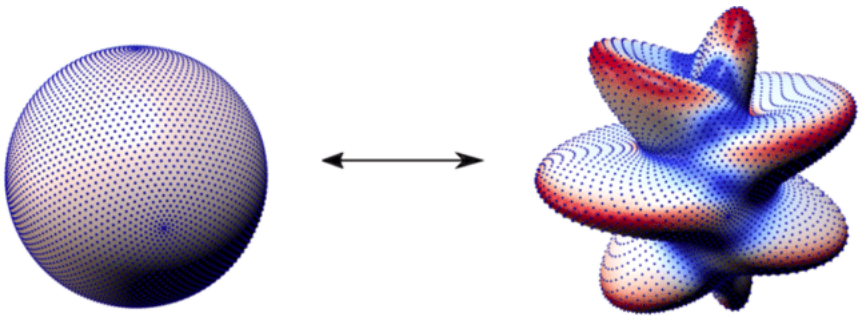

Figure IV.II: *A Lebedev sphere (showcased left), mapped onto a manifold (showcased right), where there is a new weighting function based on the local manifold metric. The Gaussian curvature of the blue area is +7 and of the red area is -7. Image from Hydrodynamic Flows on Curved Surfaces: Spectral Numerical Methods for Radial Manifold Shapes.*

Using the co-ordinates on the sphere, the Lebedev quadrature is displayed as:

$$\int_{\mathcal{S}^2} f dA = \int_0^{2\pi} \int_0^{\pi} f \sin(\phi) d\phi d\theta \tag{118}$$

$$= \sum_i f_i w_i \tag{119}$$

For the integral of the manifold (using the co-ordinates of the sphere):

$$\int_{\mathcal{M}} f dA = \int_0^{2\pi} \int_0^{\pi} f \sqrt{|g|} d\phi d\theta \tag{120}$$

$$= \int_0^{2\pi} \int_0^{\pi} f \frac{\sqrt{|g|}}{\sin(\phi)} \sin(\phi) d\phi d\theta \tag{121}$$

$$= \int_{\mathcal{S}^2} f \frac{\sqrt{|g|}}{\sin(\phi)} dA \tag{122}$$

IV.II Sparse Grids

Sparse grids are another technique to overcome the curse of dimensionality, even though the methodology is based on the evaluation of one dimensional integrals. Sparse grids carry out the quadrature of high dimensional functions by what is known as the tensor product construct, and the truncation of a multiresolution series expansion. Tensor rule ensures there will be a positive weighting function for cubature points, if a positive weighting function exists for quadrature points.

Normal grids employ the use of $\mathcal{O}(h_n^{-d})$ grid points, in order to achieve an accuracy of $\mathcal{O}(h_n^2)$. Sparse grids, utilize $\mathcal{O}(h_n^{-1} \cdot log(h_n^{-1})^{d-1})$ grid points, where h_n is the mesh width, which equals 2^{-n}, and n is the level of discretization. Sparse grids achieve an accuracy of $\mathcal{O}(h_n^2 \cdot log(h_n^{-1})^{d-1})$. Therefore, for comparable accuracy, sparse grids must utilize lesser points in a high dimensional space than regular grids.

For the composition of a sparse grid, we need to introduce a multi-index, denoted as $\underline{l}$, where $\underline{l}$ can be displayed as:

$$\underline{l} = (l_1, \ldots, l_d) \in \mathbb{N}^d \tag{123}$$

Hereafter, an anisotropic grid, $\Omega_{\underline{l}}$ on $\overline{\Omega}$ with a mesh width of $h_{\underline{l}}$, can be introduced. The mesh width remains equidistant along the grid, along the directions of each of the d dimensions.

The corresponding multidimensional space for piecewise linear functions can be displayed as

$$W_{\underline{l}} = \text{span}\{\phi_{\underline{l},\underline{j}} | j_t = 0, \ldots, 2^{l_t}, t = 1, \ldots, d\} = \text{span}\{\phi_{\underline{l},\underline{j}} | 0 \leq j \leq 2^{\underline{l}}\} \tag{124}$$

The sum of the hierarchal increment spaces produces the following function space:

$$V_l = \bigoplus_{k \leq l} W_k \tag{125}$$

The piecewise linear functions which occupy the sparse grid can be denoted as:

$$\phi_{\underline{l},\underline{j}}(\underline{x}) = \prod_{t=1}^{d} \phi_{l_t,j_t}(x_t) \tag{126}$$

where t is each coordinate direction.

The equation by which one-dimensional functions can be defined, is finally written as:

$$\phi_{l,j}(x) = \begin{cases} 1 - |x/h_l - j|, x \in [(j-1)h_l, (j+1)h_l] \cap [0,1] \\ 0 \end{cases} \tag{127}$$

which makes use of the relation $[x_{l,j} - h_l, x_{l,j} + h_l] \cap [0,1] = [(j-1)h_l, (j+1)h_l] \cap [0,1]$

We now have the piecewise linear function in one dimension, and must extend it into a mutlidimensional plane. This is done using the tensor product construct.

We use the sum of the hierarchical increment spaces, with a given multi-index, $\underline{l}$ and obtain a function space:

$$V_{\underline{l}} = \bigoplus_{k_1=1}^{l_1} \cdots \bigoplus_{k_d=1}^{l_d} W_k \tag{128}$$

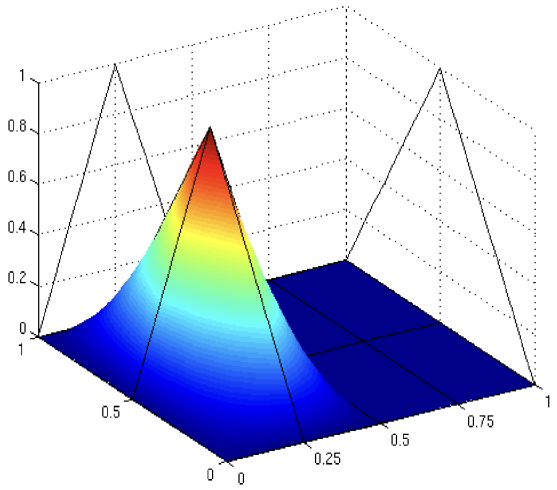

Figure IV.II: *Two-dimensional basis function* $\varnothing_{(2,1),(1,1)}$ *on the grid* $\Omega_{(2,1)}$

V_n is an isotropic space, which can be denoted as $V_n = V_{(n,\ldots,n)}$ and is a special case of (128). V_n and W_l share the following relation:

$$V_n = \bigoplus_{|l|_\infty \leq n} W_l \tag{129}$$

At last, the interpolating function of $f(x)$ can be displayed as:

$$u(x) = \sum_{|l|_\infty \leq n} \sum_{i \in I_l} \alpha_{l,i} \cdot \phi_{l,i}(x) \tag{130}$$

$$= \sum_{|l|_\infty \leq n} u_l(x) \tag{131}$$

The sparse grid quadrature rule developed by Smolyak can be displayed with a recursion formula and tensor product:

$$Q_l^{(d)} f = \left(\sum_{i=1}^{l} \left(Q_i^{(1)} - Q_{i-1}^{(1)} \right) \otimes Q_{l-i+1}^{(d-1)} \right) f \tag{132}$$

where d is the number of dimensions.

IV.III Monte Carlo

Monte Carlo is another method of numerical integration in a mutli-dimensional plane that solves the problem of the curse of dimensionality. Monte Carlo also works well with highly oscillating functions. The methodology of Monte Carlo differs from the traditional quadrature method explored thus far.

The purpose of Monte Carlo is to compute the definite integral,

$$I = \int_\Omega f(\overline{\mathbf{x}}) \, d\overline{\mathbf{x}}$$

where Ω has the volume:

$$V = \int_\Omega d\overline{\mathbf{x}} \tag{133}$$

The Monte Carlo method can be displayed as follows:

$$I \approx Q_N \equiv V \frac{1}{N} \sum_{i=1}^{N} f(\overline{\mathbf{x}}_i) = V \langle f \rangle \text{ as } \lim_{N \to \infty} Q_N = I \tag{134}$$

References

[AW] Branden Archer and Eric W. Weisstein. "lagrange interpolating polynomial." from mathworld–a wolfram web resource. Last visited on 16/7/2023.

[Bai06] David H. Bailey. Tanh-sinh high-precision quadrature. 2006.

[BFB15] Richard L Burden, J Douglas Faires, and Annette M Burden. *Numerical analysis*. Cengage learning, 2015.

[BS17] Johannes Brumm and Simon Scheidegger. Using adaptive sparse grids to solve high-dimensional dynamic models. *Econometrica*, 85:1575–1612, 09 2017.

[Cha13] Subrahmanyan Chandrasekhar. *Radiative transfer*. Courier Corporation, 2013.

[GA18] B.J. Gross and P.J. Atzberger. Hydrodynamic flows on curved surfaces: Spectral numerical methods for radial manifold shapes. *Journal of Computational Physics*, 371:663–689, oct 2018.

[Gar13] Jochen Garcke. Sparse grids in a nutshell. In *Sparse grids and applications*, pages 57–80. Springer, 2013.

[Hil87] Francis Begnaud Hildebrand. *Introduction to numerical analysis*. Courier Corporation, 1987.

[Kre] Kevin Kreider.

[Pet] Janet Peterson.

[Ron16a] Amos Ron, Oct 2016.

[Ron16b] Amos Ron, Oct 2016.

[Smo63] Sergei Abramovich Smolyak. Quadrature and interpolation formulas for tensor products of certain classes of functions. In *Doklady Akademii Nauk*, volume 148, pages 1042–1045. Russian Academy of Sciences, 1963.

[Sze39] Gabor Szeg. *Orthogonal polynomials*, volume 23. American Mathematical Soc., 1939.

[VSM20] Joren Vanherck, Bart Sorée, and Wim Magnus. Tanh-sinh quadrature for single and multiple integration using floating-point arithmetic, 2020.

[Weia] Eric W. Weisstein. "cavalieri's quadrature formula." from mathworld–a wolfram web resource. Last visited on 16/7/2023.

[Weib] Eric W. Weisstein. "chebyshev-gauss quadrature." from mathworld–a wolfram web resource. Last visited on 16/7/2023.

[Weic] Eric W. Weisstein. "gaussian quadrature." from mathworld–a wolfram web resource. Last visited on 16/7/2023.

[Weid] Eric W. Weisstein. "hermite-gauss quadrature." from mathworld–a wolfram web resource. Last visited on 16/7/2023.
[Weie] Eric W. Weisstein. "laguerre-gauss quadrature." from mathworld–a wolfram web resource. Last visited on 16/7/2023.
[Weif] Eric W. Weisstein. "radau quadrature." from mathworld–a wolfram web resource. Last visited on 16/7/2023.
[Wei00] Stefan Weinzierl. Introduction to monte carlo methods, 2000.
[Wik21] Wikipedia contributors. Gauss–laguerre quadrature — Wikipedia, the free encyclopedia, 2021. [Online; accessed 16-July-2023].
[Wik22a] Wikipedia contributors. Cavalieri's quadrature formula — Wikipedia, the free encyclopedia, 2022. [Online; accessed 16-July-2023].
[Wik22b] Wikipedia contributors. Clenshaw–curtis quadrature — Wikipedia, the free encyclopedia, 2022. [Online; accessed 16-July-2023].
[Wik22c] Wikipedia contributors. Gauss–hermite quadrature — Wikipedia, the free encyclopedia, 2022. [Online; accessed 16-July-2023].
[Wik22d] Wikipedia contributors. Lebedev quadrature — Wikipedia, the free encyclopedia, 2022. [Online; accessed 16-July-2023].
[Wik23a] Wikipedia contributors. Euler–maclaurin formula — Wikipedia, the free encyclopedia, 2023. [Online; accessed 16-July-2023].
[Wik23b] Wikipedia contributors. Fourier sine and cosine series — Wikipedia, the free encyclopedia, 2023. [Online; accessed 16-July-2023].
[Wik23c] Wikipedia contributors. Gauss–kronrod quadrature formula — Wikipedia, the free encyclopedia, 2023. [Online; accessed 16-July-2023].
[Wik23d] Wikipedia contributors. Gauss–legendre quadrature — Wikipedia, the free encyclopedia, 2023. [Online; accessed 16-July-2023].
[Wik23e] Wikipedia contributors. Monte carlo integration — Wikipedia, the free encyclopedia, 2023. [Online; accessed 16-July-2023].
[Wik23f] Wikipedia contributors. Simpson's rule — Wikipedia, the free encyclopedia, 2023. [Online; accessed 16-July-2023].
[Wik23g] Wikipedia contributors. Sparse grid — Wikipedia, the free encyclopedia, 2023. [Online; accessed 16-July-2023].
[Wik23h] Wikipedia contributors. Spherical harmonics — Wikipedia, the free encyclopedia, 2023. [Online; accessed 16-July-2023].
[ZH91] Christoph Zenger and W Hackbusch. Sparse grids. In *Proceedings of the Research Workshop of the Israel Science Foundation on Multiscale Phenomenon, Modelling and Computation*, page 86, 1991.

[Hil87] [Cha13] [GA18] [Wei00] [BS17] [Gar13] [ZH91] [Smo63] [Wik23f] [Weic] [Bai06] [VSM20] [Sze39] [AW] [Weif] [Weib] [Weia] [Wik22d] [Wik23e] [Wik23h] [Wik23a] [Wik22a] [Wik22b] [Wik23b] [Weie] [Weid] [Wik23c] [Wik22c] [Wik21] [Wik23d] [Wik23g] [Ron16a] [Ron16b] [BFB15] [Kre] [Pet]

Email address: vrhea@tisb.ac.in

Euler Circle, Mountain View, CA 94040